

FLOW CHARACTERISTICS AT THE RIP CURRENT NECK UNDER LOW ENERGY CONDITIONS

D. BOWMAN¹, D. S. ROSEN², E. KIT², D. ARAD¹ and A. SLAVICZ²

¹Department of Geography, Ben-Gurion University of the Negev, Beer-Sheva 84105 (Israel)

²Coastal and Marine Engineering Research Institute, Technion City, Haifa 32000 (Israel)

(Received February 23, 1987; revised and accepted August 4, 1987)

Abstract

Bowman, D., Rosen, D.S., Kit, E., Arad, D. and Slavicz, A., 1988. Flow characteristics at the rip current neck under low energy conditions. *Mar. Geol.*, 79: 41–54.

This paper presents the flow signature of the rip current neck as determined by fourteen near-bottom velocity records, with a comparison made to 63 recordings in the surf zone. The field experiments, including wave monitoring and morphological mapping, were conducted under relatively calm, dissipative wave conditions ($T_{sig} = 3-6$ s, $H_{sig} = 0.3-1.1$ m) at Herzliya beach, Israel, on the Mediterranean shore. The current data were analysed for shore-normal and resultant components. The processing of the time series in the form of instantaneous and smoothed velocities, provided spectral energy, orbital and current velocity, specific current discharge and directional distribution data.

The unique characteristic of the neck environment was found to be its continuous unidirectional seaward flow. Due to the channeling effect, this steady offshore drift constituted the fastest flow in the surf zone with a typically narrow ($35^{\circ}-94^{\circ}$) directional range. Through spectral analysis of the unidirectional return flow the morphodynamic process signature at the rip neck was defined by the relative contribution from the incident waves (78%), the subharmonic edge waves (14%) and the infragravity oscillations (8%). The pulsatory, jet-like rip model with concentration of energy at low frequencies is not corroborated by this study. The studied environment of the rip and bar pattern represented an inherited beach morphology, at an initial accretional, although not yet reflective, stage.

Introduction

Many investigators have addressed the rip flow phenomenon (e.g., Basco, 1982). However, there have been relatively few rip current field experiments reported. The first detailed near-shore circulation measurements were reported by Shepard and Inman (1950). Sonu (1972), by means of weighted floats, dye, balloon photographs and bidirectional propeller-type current meters, produced evidence of velocity variations occurring along rips. He studied the vertical velocity profiles and showed that from the feeder channels seaward, the position of maximum velocity in the profile moved up-

wards. Davidson-Arnott and Greenwood (1974), observed in a barred inshore with 2–3 m high waves and a $T = 4-5$ s, rips with speeds of 0.5–0.75 m/s. Rip currents were also noted by Clifton (1976) and deduced from offshore-dipping structures observed in core peels by Davidson-Arnott and Greenwood (1976), Greenwood and Davidson-Arnott (1979) and by Lenhart (1979). Greenwood and Hale (1980) reconstructed rip-type currents from the seaward-dip of medium-scale trough cross-stratification on bars. Long-term daily rip current observations accompanied by wave climate data were undertaken by Short (1985).

Shepard and Inman (1950) showed that

longshore currents transforming into rips increased in mean velocity from 0.25 m/s to 1.0 m/s. Wright et al. (1986) reported that flow was seaward at all depths within the rip. Maximum rip velocity in the surf, as well as in rough sea conditions, was reported to be in the range of 1–2.5 m/s (Shepard et al., 1941; Draper and Dobson, 1965; Cook, 1970; Wright, 1982; Basco, 1983). This is generally comparable to the maximum rip current velocities of 1.8 m/s calculated by stream function solutions for oblique wave incidence (Noda, 1974).

The flow characteristics of rip currents, i.e., velocity–time asymmetry, unidirectionality and pulsatory behavior, have, however, not

been investigated in detail. This paper results from a detailed field experiment, aimed at studying the near-bottom velocity signature of the rip system by direct field measurements on the southeastern Mediterranean coast of Israel. In our paper we have focused on the distinct site of the rip channel proper, or rip neck environment, located within oblique–transverse bars.

Study area

The study site at Herzliya is located on the Mediterranean, north of Tel Aviv (Fig.1). It is a straight, plan-shaped, medium sized sandy

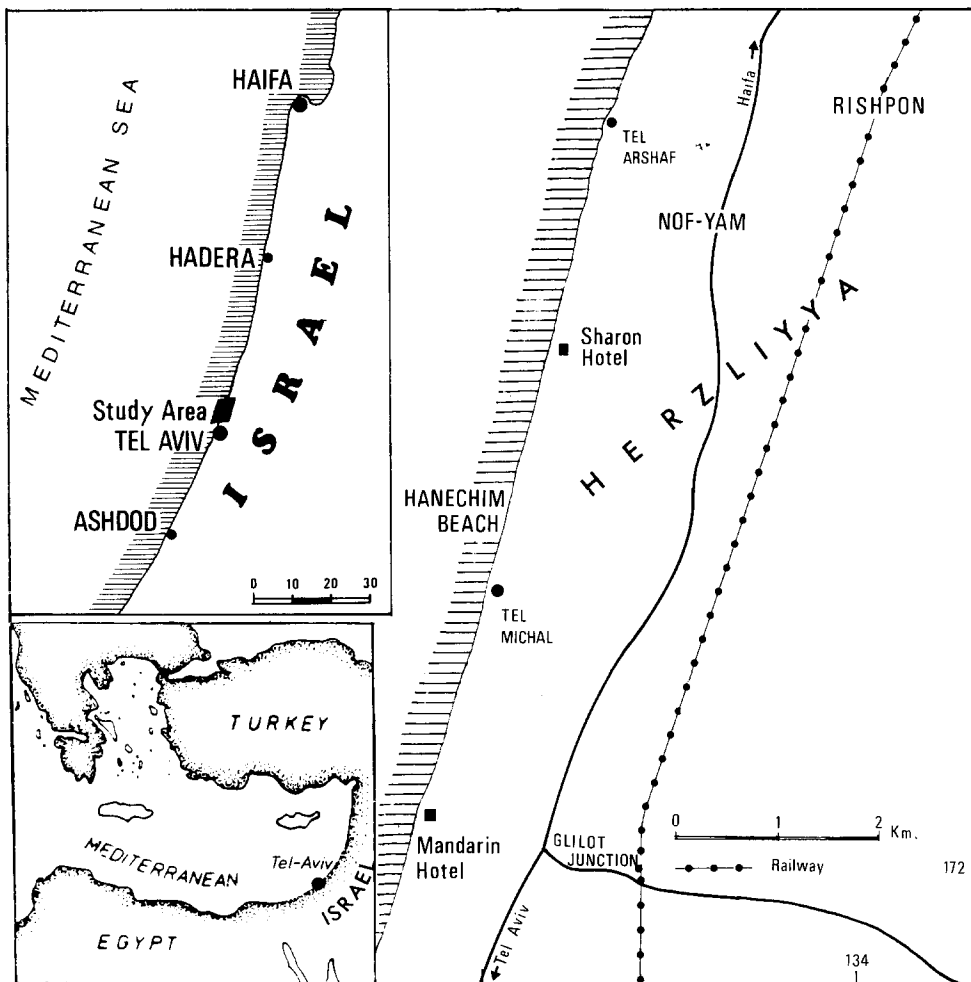


Fig.1. Location maps.

beach, oriented N13°E, uniformly sloping 0.6°–1.3° and backed by a coastal eolianite cliff. The study area experiences a microtidal range averaging less than 50 cm. Wave breaking is predominantly in the spilling range. The prevailing wave characteristics during the study period were: $H_{sig} = 0.3\text{--}1.1$ m, $H_{max} = 0.4\text{--}1.9$ m and $T_{sig} = 3\text{--}6$ s, with a W–WNW incident wave direction, all of which are typical of the summer conditions.

The modal beach state and the energy-environmental characteristics were summed up by the dimensionless parameter (Dean, 1973) $\Omega = H_b/TW_s$, where H_b is the breaker height, T is the peak breaker period and W_s is the fall velocity of the beach sediment. The instantaneous Ω values ranged from 3 to 4, indicating an intermediate beach state with erosional ($\Omega > 2.5$) rips (Short, 1985). The rips alternate within megacusp embayments, between well-developed transverse and oblique rhythmic bars in an accretionary sequence, forming skewed and normal circulation cells, analogous to the connected inner bar systems of Greenwood and Davidson-Arnott (1975). The horizontal rip cell segregation is typical of beaches in the intermediate state (Wright et al., 1982). The transverse bar and rip beach state and the associated instantaneous Ω parameter may indicate, following Wright and Short (1984) and Wright et al. (1985), a stable to near-equilibrium state.

Additional information may be obtained by applying the surf scaling parameter ϵ for defining the morphodynamic beach state (Guza and Inman, 1975). The equation for ϵ is $= a_i w_i^2 / g \tan^2 \beta$, where a_i = incident wave amplitude near the point of wave breaking, $w_i = 2\pi/T$ (where T = wave period), g = acceleration of gravity and β is the inshore–foreshore slope. The rip embayment manifested a dissipative ($\epsilon > 33$) to transitional ($\epsilon = 6$) beach state, whereas the rip neck was extremely dissipative ($\epsilon \gg 33$). The low-level accretionary stage in our study area, i.e., the lack of fully-developed summer profiles and of a steep beach face, associated with a medium grained sediment, are held responsible for the dissipativeness.

Data base

Field data

Field data were collected twice monthly from March to October 1983. Each day of field work started with a flight over the study area for observation and photography. Two bidirectional, 4 cm sensor diameter electromagnetic current meters (type M-512 of Marsh–McBirney), with time constants of 0.5 s, were shifted from one recording station to the next in the surf zone, along and across the rip channels and the nearshore bars, resulting in a total of 63 monitored sites. The calibration uncertainty associated with these flowmeters is in the 5–10% range (Cunningham et al., 1979; Guza and Thornton, 1980; Basco, 1982). The dependence on turbulence properties was not studied (Aubrey and Trowbridge, 1985). Near-bottom currents were recorded with the sensing elements mounted at $Z = 36$ cm above the bed. In two thirds of the recordings, the elevation of the sensors was within the lower third of the water column. In one third of the stations the sensors in shallower waters were positioned relatively higher, but still below mid-depth.

In order to record the orthogonal, shore-normal (U) and longshore (V) horizontal components, the currentmeters were installed in a N13°E orientation which had been determined by compass measurements and maintained with pins fixed into the sea bed. The sensors were hard wired to the beach and logged on a multichannel A/D magnetic tape cassette datalogger and simultaneously chart-recorded. Data were scanned by a multiplexer at the rate of 1.875 Hz/channel. Ten tape malrecorded stations were digitized from the paper chart records and logged on a magnetic tape in the same format. Bathymetric data were obtained from survey lines to the limit of the wading depth, using level and staff. Long-term time series of significant wave heights and periods, at 3 h intervals, were obtained by offshore Datawell wave riders, monitoring at Hadera, 33 km north of the study site, and at Ashdod, 40 km south of Herzliya.

Data processing

The time series of the currents forming the primary data base were processed to define their characteristic flow signatures. Each recording was cut to 2048 data points, representing 1024 s of record length, and was read by a cassette reader connected to a minicomputer system. High-frequency oscillatory velocities were separated out by the "running average" filtration method. A cosine window, 18.5 s wide, was applied to remove shorter than subharmonic orbital incident velocities. The resulting signals, after filtration, were regarded as being generated mainly by tidal, longshore, rip and general circulation currents. The processing involved time series of the instantaneous velocity, including waves and currents, and the net direct current ignoring the orbital motion. Flow asymmetry was analysed with respect to both magnitude and duration and was also shown as the cumulative offshore- and onshore-directed discharges. The time-averaged current vector, including amplitude and orientation and the velocity distribution of the vector and the directional distribution of each record were also computed (Kit et al., 1985). The following groups with their respective directional range were defined: A=excellent concentration of flow, $<60^\circ$, B=good concentration, $60^\circ\text{--}120^\circ$, C=poor concentration, $120^\circ\text{--}240^\circ$ and flow divergence, $240^\circ\text{--}360^\circ$.

The energy spectra were computed by the fast Fourier transform including the peak period for each spectra distribution, with the low frequency cut at 1/180 s. The frequency range was divided into three domains, as follows: (1) The domain attributed to infragravity waves corresponding to the frequency range $<1/5 T_p$, where T_p is the spectral peak, (2) the frequency range attributed to subharmonic edge waves corresponding to the frequency range $1/1.5 T_p\text{--}1/5 T_p$, and (3) the frequency range usually corresponding to gravity waves in the $0.4\text{--}1/1.5 T_p$ range. In order to infer wave heights at each recording station, and to obtain time series of the sea

surface elevation, the linear wave theory transfer function was applied to the velocity measurements.

Daily bathymetric maps were prepared by manual interpolation of the leveling data, with the aid of the overflight observations and the field notes. Each recording station was environmentally defined according to its location characteristics and the following inshore subenvironments were obtained: oblique and parallel bars, shore-parallel channels, the upper, most shallow feeder segment, the wider and deeper segment of the feeder, the rip channel neck, the deepest rip segment off the oblique-transverse bars, and morphologically undefined surfaces on the inshore, sloping offshore.

The shifting of flowmeters during each field experiment from one recording site to the next could have resulted in superposition of temporal, daily wave changes on the spatial environmental characteristics, i.e., substitution of space by time. However, the daily range of the significant wave (8–24 cm), was low and unrelated to the spatial trends, suggesting that the daily wave fluctuation factor could be ignored and the current records regarded as time-independent.

Results

Main flow signatures

The neck shows an extreme flow asymmetry offshore, i.e., whereas the feeders showed the mean onshore-offshore peaks to be almost balanced at 82 and 95 cm/s respectively, the mean onshore-offshore peaks at the necks were 67 and 132 cm/s respectively. However, what is even more unique about the records of the neck is their continuous offshore-directed flow (Fig.2), i.e., not their net time-averaged unidirectionality, which is typical of asymmetric oscillatory flows, but their almost uninterrupted offshore unidirectional drift, which is a main flow signature of the rip neck. Some of the instantaneous velocity records showed short periods of onshore flow, i.e.,

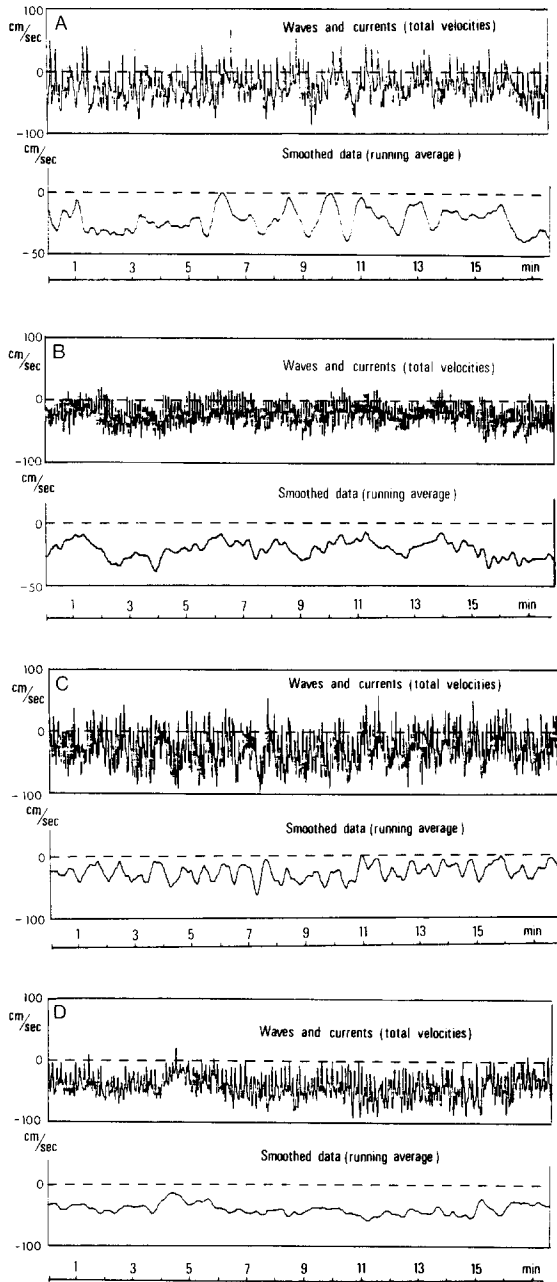


Fig. 2. Typical time series recordings at the rip neck. Upper graphs show total waves and currents with instantaneous shore-normal velocities. Lower graphs show smoothed shore-normal current data, based on the running average. Positive values indicate onshore direction. A. 26/9/83. Station 3. Depth=1.2 m; $H_{sig}=1.0$ m; $T_{sig}=4$ s; mean $v = -22.1$ cm/s. B. 30/5/83. Station 7. Depth=1.38 m; $H_{sig}=0.34$ m; $T_{sig}=4$ s; mean $v = -21.3$ cm/s. C. 16/5/83. Station 3. $H_{sig}=0.7$ m; $T_{sig}=5$ s; mean $v = -26.5$ cm/s. D. 25/9/83. Station 4. Depth=1.31 m; $H_{sig}=0.65$ m; $T_{sig}=5$ s; mean $v = -40$ cm/s.

preservation of the onshore-directed orbital components. In other cases (Fig.2D) even the instantaneous data were almost continuously offshore-directed, i.e., the superimposed orbital motion did not influence the dominant offshore direction and was expressed by velocity fluctuations only.

Continuous unidirectional neck flow was located in two typical sites within the surf zone. Figure 3A shows the site in oblique rip channels at the deepest surf position closest to the breakers, and Fig.3B shows the sites closer to the shore, towards which two feeders converge to form a transverse rip. The typical cross-sectional geometry of such channels was as follows: A 15–35 m width and a 1–2 m water depth, of which 50–70 cm have been entrenched below the surrounding bed. Contrary to most rip studies in which the neck was observed at, or off the breakers, in our study, because of the low predominant waves, the neck occurs mainly within the surf zone.

Flow velocities

Under the prevailing calm wave conditions and the barred bathymetry in the study area, velocities of the unidirectional return flow ranged between 25 and 55 cm/s. These velocities were equivalent to the fastest onshore surges associated with incident waves, and composed the strongest flows recorded in the entire inshore (Fig.4). Maximum orbital velocities recorded on the exposed flanks of the nearshore bars ranged from 41 cm/s to 66 cm/s compared to similar maximum velocities of the rip current. The relatively high velocity of the unidirectional return flow is best manifested by the water flux parameter, which constitutes the offshore specific discharge and integrates the instantaneous velocity fluctuations accumulated over an entire record. Figure 5 indicates that the unidirectional return flow attained the highest discharge within the surf zone. Figure 6 demonstrates the fading out of the velocity of the return flow across the rip neck from the center of the channel towards the margins.

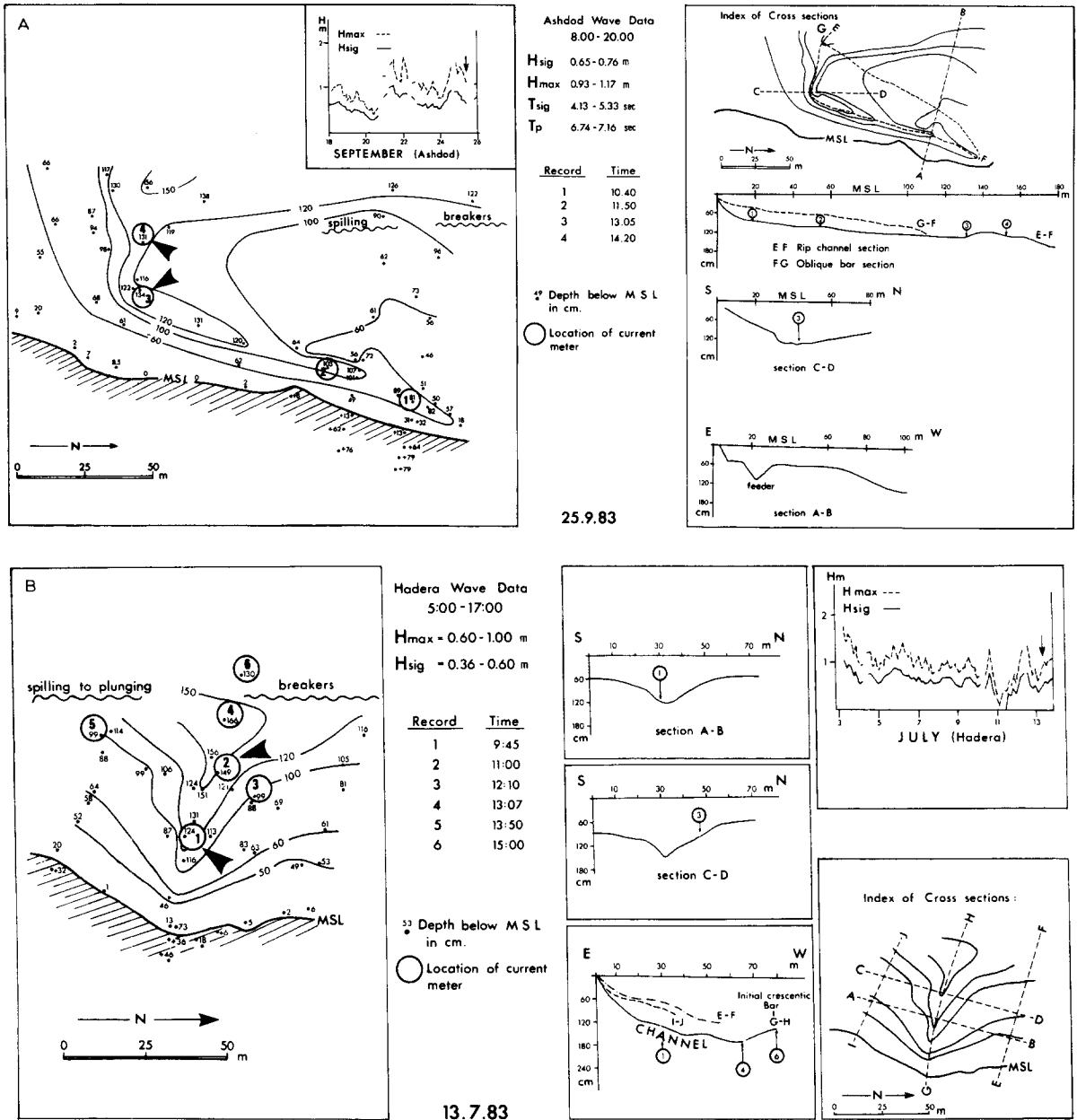


Fig.3. Typical sites of the continuous return flow (indicated by bold arrows) at Herzliya beach. A. 25/9/83. The deepest surf site by the breakers in an oblique rip system. B. 13/7/83. Close to the swash zone at an almost transverse rip channel. Wave data and cross sections are also shown.

In spite of the calm conditions, and because of the efficient channeling effect, the unidirectional return current attained at the neck, flow velocities equivalent to, or faster than, the incident orbital motion. Continuity was achieved within the coastal cell only by

forcing the water out through the rip neck with the highest surf zone velocities. Wright and Short (1984) concluded that the transverse bar and rip state produce the strongest rip for any given breaker height.

Flow stability at the neck is manifested by

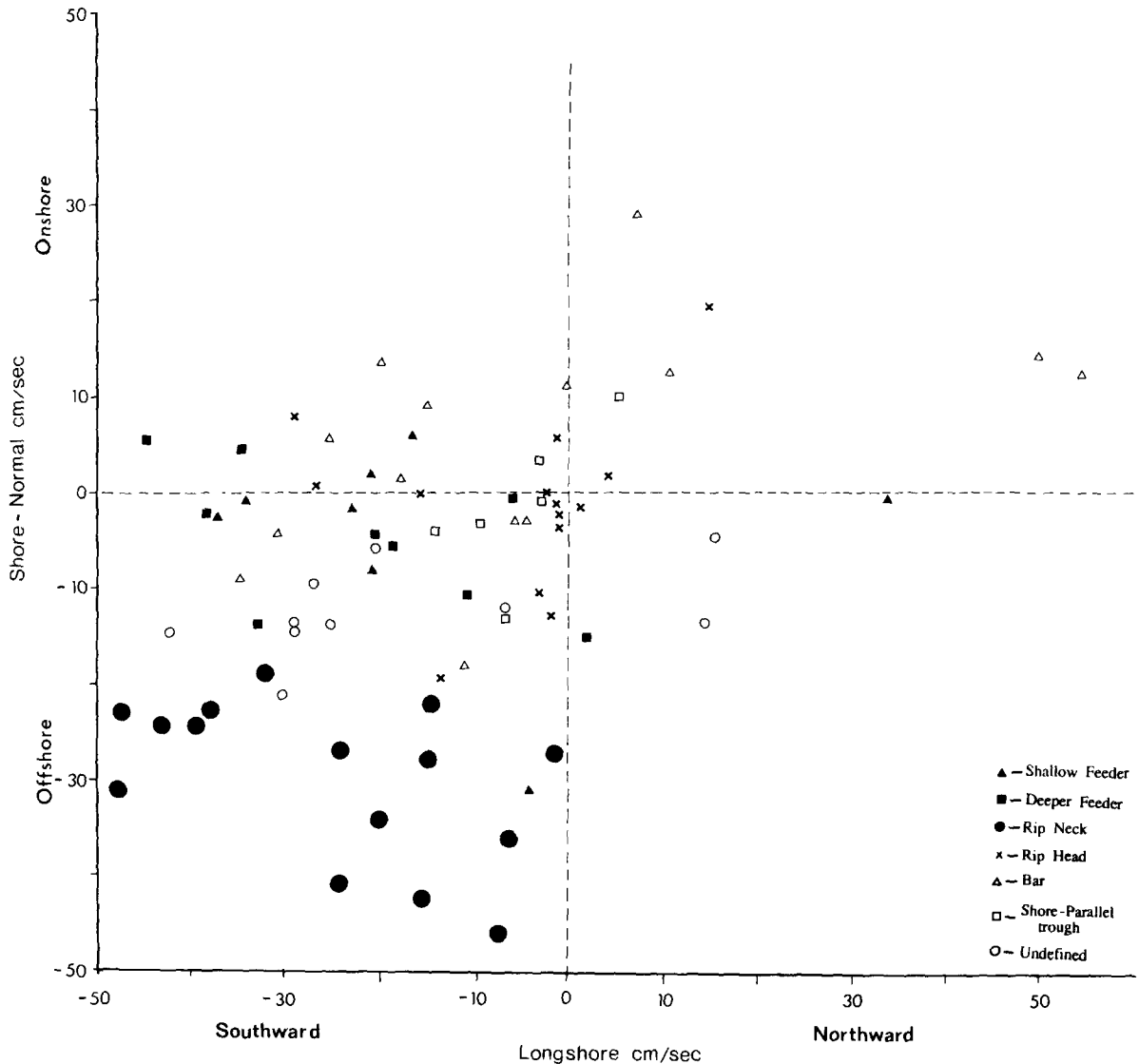


Fig.4. Current data (waves and currents) at various subenvironments in the surf zone resolved into mean longshore and mean shore-normal components. The rip neck values indicate the peak shore-normal velocities. Undefined values indicate inshore surfaces, sloping offshore.

the relative low velocity standard deviation compared to other sites in the surf zone (Fig.7). The range of the velocity fluctuations along the rip system is negatively related to the velocity amplitude: It is low — 25.2–55.1 cm/s — in the neck, compared, for example, to 5.6–43.6 cm/s in the feeders. Numerical solutions in earlier work (Arthur, 1962; Bowen, 1969), based on nonlinear inertial terms, indicated the convergence of streamlines toward

the rip current neck. Previous studies also showed that the effect of rip current and wave interaction is to oppose rip current outflow and reduce its velocity (Leblond and Tang, 1974).

From the point of view of sediment transport, the mean sediment size in the study area (0.272 mm), falls within the zone of “minimum erosion velocity” (Hjulstrom, 1935). The threshold velocity for these sediments is, according to Komar and Miller (1975), in the

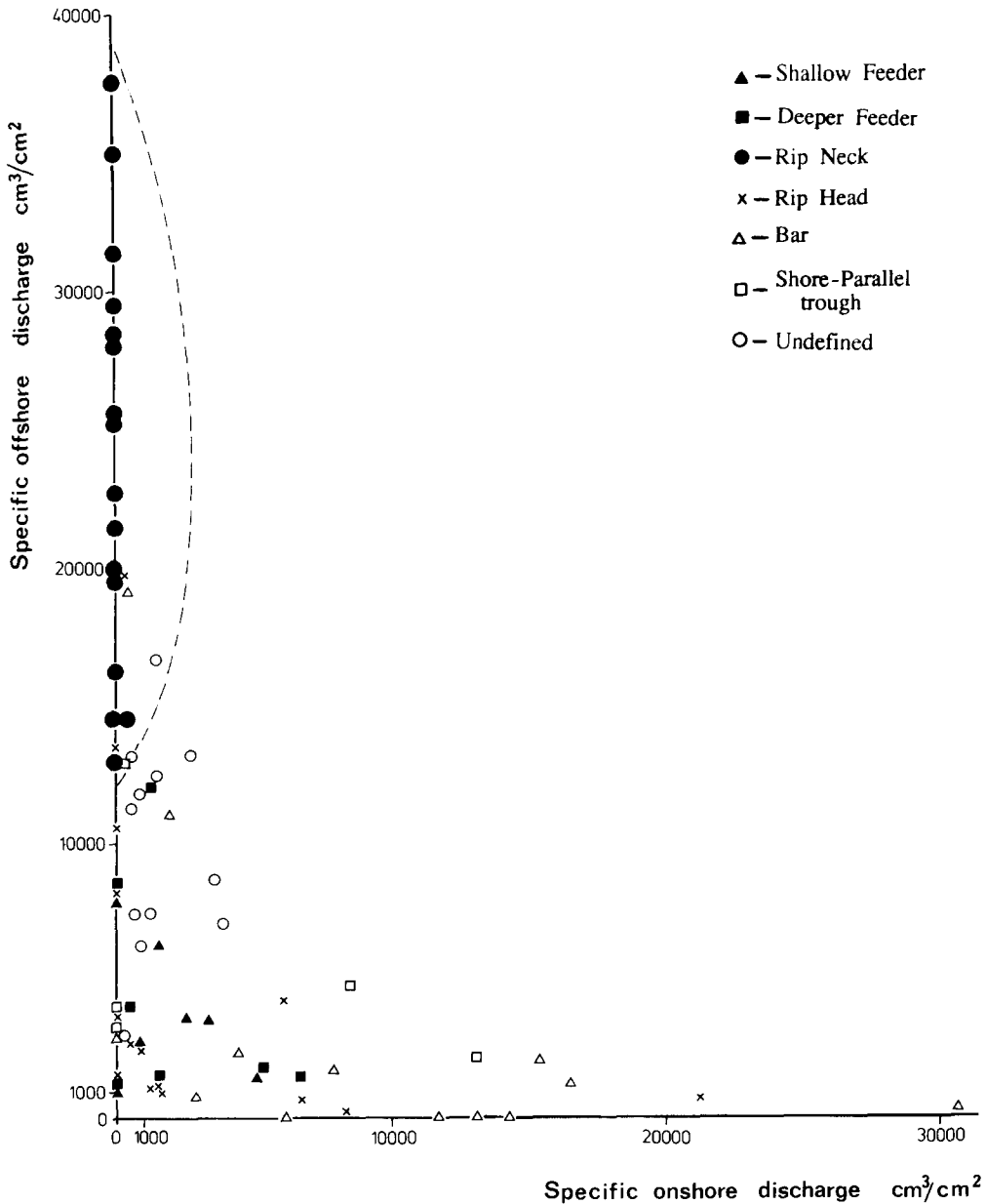


Fig.5. Onshore versus offshore specific discharge at various subenvironments in the surf zone, based on smoothed data and calculated for a flow through a cross section of 1 cm² over an entire record. The unidirectional return flow at the neck (broken line) indicates the largest specific discharges.

range of 20–25 cm/s. The current velocities thus exceeded the threshold of motion. Figure 8 demonstrates, in the surf zone, the time percentage of the total current, including waves, above the 20 cm/s threshold velocity. No clear environmental grouping is revealed here. However, the mean percentage of time

above threshold velocity is highest at the neck (94%); that of the feeder is at 74%, whereas the head, with 26%, clearly reflects the decaying phase. The rip neck environment characteristically falls outside the wave height–current velocity correlation field (Fig.8), indicating its second-order nature and its independence

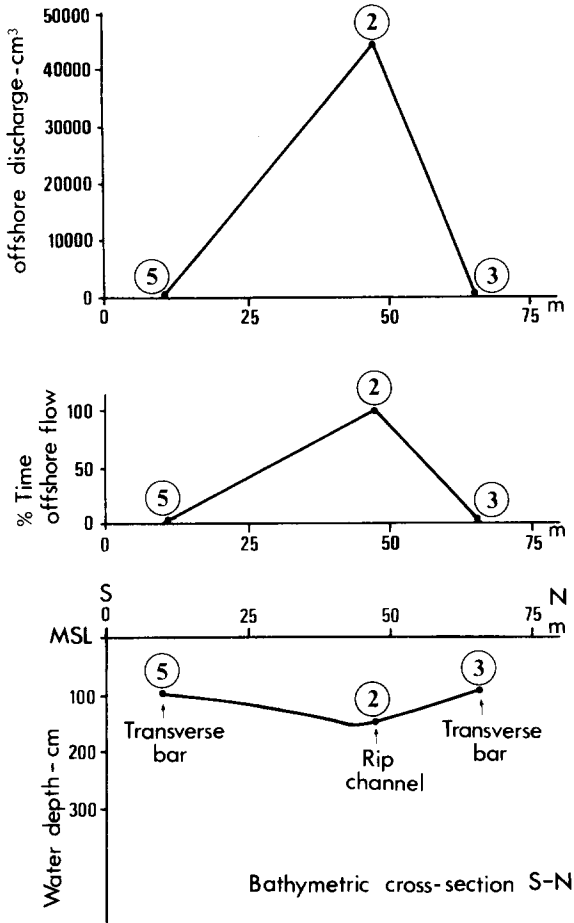


Fig.6. Velocities of the return flow across the neck on 13/7/83, indicating decay towards the margins. The bathymetry of the site is shown in Fig.3. Encircled numbers indicate current meter locations.

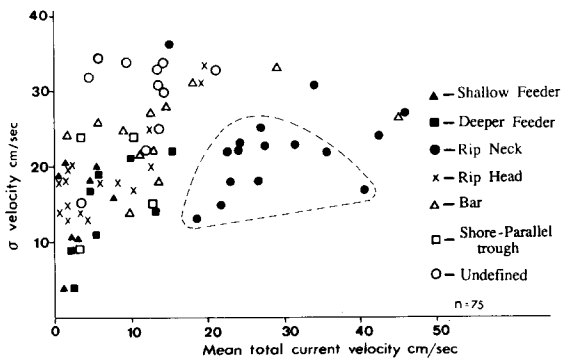


Fig.7. Standard deviation of the total current velocities (waves and currents) at various subenvironments in the surf zone. Note the relatively low standard deviation of the return flow (encircled).

of the waves which directly approach the neck.

The flow in the neck possesses a typically narrow directional range 35° – 94° (Fig.9A–C). A rip neck located at the convergence site of two feeders demonstrated a wider directional range (Fig.9D) and a rip feeder influenced by lateral currents showed an even wider directional range (Fig.9E). The flow at the neck seems to owe its relative narrow directional band both to the channeling effect and to the relatively high velocities which cause the concentration of streamlines.

Spectra of current oscillations

Subharmonic edge waves have been consistently reported for reflective beaches and rip embayments (Huntley and Bowen, 1975; Guza and Inman, 1975; Wright et al., 1979a). For gently sloping beaches the frequencies reported were much lower than those of the incoming waves (Huntley and Bowen, 1973). The energy spectra of the unidirectional return flow (Fig.10) indicates concentration of energy in the gravity range (Table 1). The oscillations associated with the incident wave frequency are the most dominant at the neck. No significant low-frequency energy peak, which could have expressed surf beat pulsation, has been detected. Most spectra contain a single significant primary peak with a rapid decay towards a minor peak at lower frequencies (Fig.10, zones A, B and C), a feature also manifested by strong rips (Wright and Short, 1984). The relative magnitudes of the subharmonic and infragravity oscillations versus the incident wave currents suggest that, at the neck, incident wave energy is far more important compared to the surf beat. Along rip systems, some subharmonic energy — twice the period of the incident waves — was consistently observed in the feeder, but it diminished towards the rip neck (Bowman et al., in prep.). The degree of dissipation at the rip neck corresponds to its relative low subharmonic energy (Table 1). The transverse bar and rip state is usually distinguished by reflective

TABLE 1

Spectra characteristics of the unidirectional return flow at the rip neck compared to the feeder. The relative magnitudes of the different modes of motion are indicated. T_p indicates peak period

Period range	$> 5T_p$		$1.5-5T_p$		$2.5s-1.5T_p$	
Main energetic domain	A		B		C	
	Infragravity		Subharmonic		Gravity	
Environment	Rip feeder	Rip neck	Rip feeder	Rip neck	Rip feeder	Rip neck
Range (%)	2-18	3-14	7-56	7-36	33-86	55-86
Mean (%)	8	8	30	14	62	78

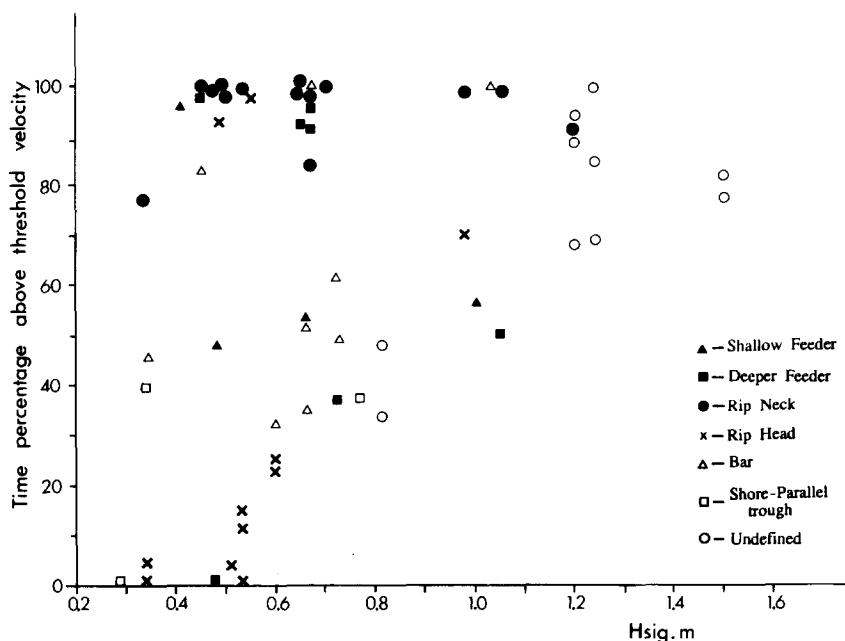


Fig.8. Percentage of time with currents above threshold velocity (> 20 cm/s) related to the incident wave height (H_{sig}). The unidirectional return flow is the only subenvironment where velocity is totally unrelated to the wave height.

rip embayments (Wright and Short, 1983). Strong, large-scale rips under dissipative conditions have been observed by Short (1979) and Wright et al. (1979b) during storms, i.e., under very different beach conditions compared to ours.

Discussion and summary

The data suggest that, within the studied rip current system, which is a seasonal, or even

intraseasonal phenomenon, the offshore-directed flow asymmetry reaches its peak at the rip neck where it is transformed into a unidirectional continuous return flow. Surf beat frequencies account for less than 10% of the energy spectra. The near-bottom currents are dominated by incident wave oscillations. Similar lack of low-frequency energy in the surf zone has been reported by Greenwood and Sherman (1984) and by Wright et al. (1986), who related the suppression of the low-frequency waves to

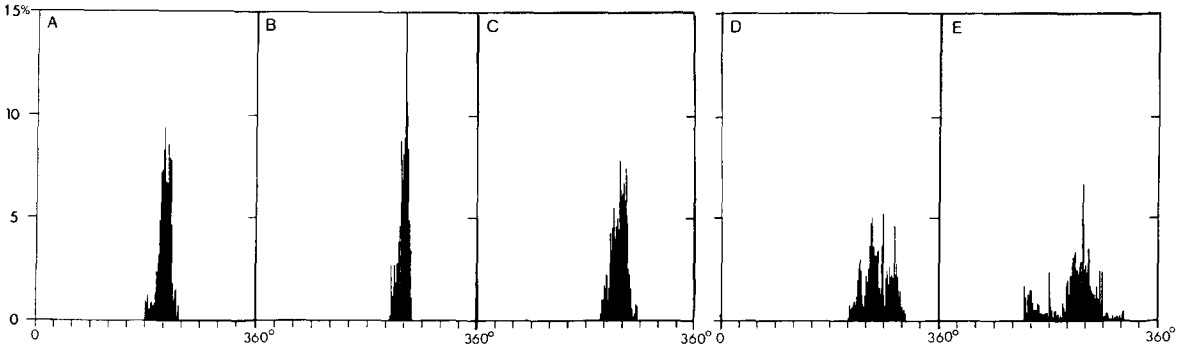


Fig.9. Examples of directional distribution of currents. A-C. Typical unidirectional rip neck flow in an oblique channel. D. Wider unidirectional rip neck flow located at the convergence site of two feeders. E. A rip feeder influenced by lateral onshore wave incident currents.

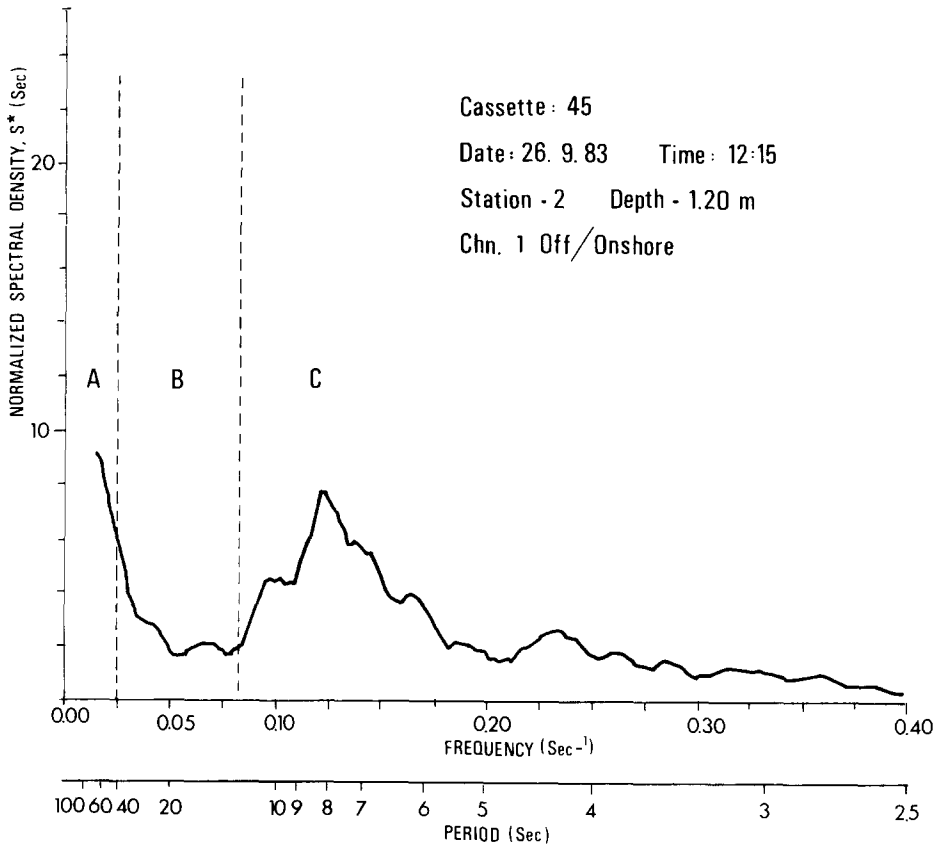


Fig.10. Major spectral features of the unidirectional return flow corresponding to Table 1. Note the dominance of the incident wave frequency (C). B—subharmonic mode; A—infragravity mode.

the inshore bar system. The pulsatory, jet-like rip model (Short, 1985) having a 5–10 min average lifespan with a concentration of energy at the lower frequencies and regulation by the

surf beat (Cook, 1970; Vos, 1976; Holman, 1981; Wright, 1982; Short, 1985) is neither confirmed by our spectra data nor by the continuous offshore-directed smoothed velocity records.

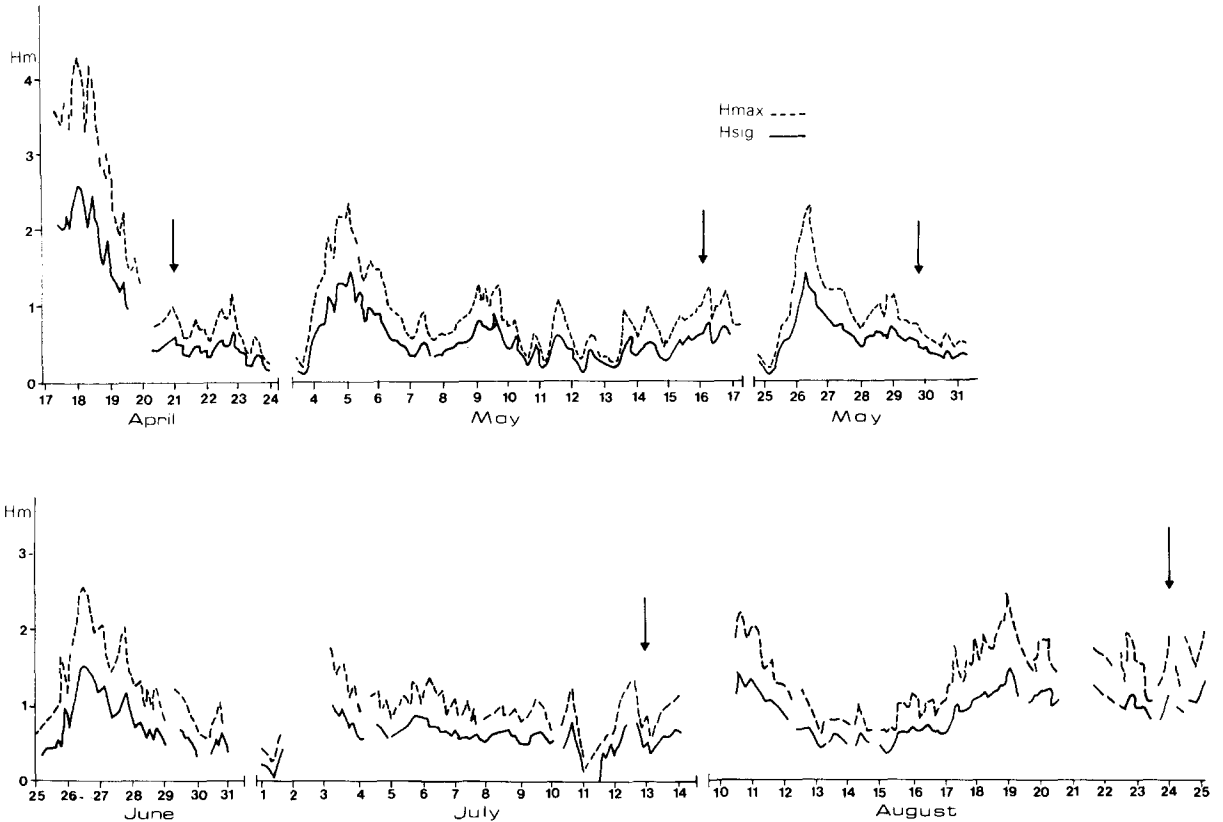


Fig.11. Wave history prior to some of the field experiments (arrows). The calm intervals indicate antecedent morphology.

From bar studies along the Israeli Mediterranean coast it has been concluded (Goldsmith et al., 1982) that the response time of the oblique-transverse beach state is in the scale of weeks after a storm, before the bottom morphology is reshaped and the initial crescentic bar pattern takes over. This corresponds to the period of calm conditions which is out of phase with the morphology as represented by this study (Fig.11). The alternating transverse and oblique bar pattern at the study area manifests antecedent processes, driven by the summer storms, which are superimposed on the summer accretional trend (Bowman, 1981). The channeled beach morphology and the relative low-flow velocity suggest that the studied bar and rip stage reflects an inherited morphology, still at its initial accretional stage, and outside the reflective domain. These characteristics are suggestive of an initial

substage of the intermediate accretional transverse bar and rip state, described by Wright and Short (1984).

The wave conditions under which this study was undertaken represent over 60% of the wave climate along the Israeli coast and show that under such conditions, with storms separated by calm intervals (Fig.11), distinct dissipative rip necks persist throughout the low-energy periods without becoming underfit. This is true not only because of a lack of energy available for changing the morphology (Wright, 1982), but primarily because of sufficient available power for maintaining the arrested position of the channel by inhibiting infilling. The rips did not widen to form less concentrated streamlines under low surf conditions, i.e., the necks did not become obscure as suggested by Sonu (1972). Furthermore, the neck environment did not show the lowest

longshore velocity recorded by Sasaki and Horikawa (1975) over rip channels.

Under the studied low-level accretional beach conditions, wave energy still allowed the continuous unidirectional return flow to operate, but only along a narrow segment. Neither feeders nor rip heads were occupied by such a unidirectional return flow. It is suggested that this study reflects a near-threshold state, i.e., higher waves would supposedly have lengthened the continuous return flow segment and a decrease in wave energy would have formed a reflective beach without rips (Short, 1985). Such transformational states still await further study. Future rip studies should, among others, aim towards examining the sequential development of rips from the high energy state with wide unchanneled currents, through a fully unidirectional channeled state, to a partly unidirectional "neck-limited" state, as has been encountered by the present study. Such a sequence is supposedly connected with the gradual integration of small rips into bigger systems (McKenzie, 1958; Short, 1985).

Acknowledgements

This study was fully supported by the Earth Science Research Administration of the Ministry of Energy and Infrastructure. The Coastal and Marine Engineering Research Institute, Haifa, provided half of the data processing costs. The help of Prof. Ben-Yaaqov of the Department of Electrical and Computer Engineering, Ben-Gurion University of the Negev, is highly appreciated. Thanks also go to V. Goldsmith for his constructive critical review, to Mrs Sharona Lazar for the drafting work and to Mrs Sonia Oren for the typing.

References

- Arthur, R.S., 1962. A note on the dynamics of rip currents. *J. Geophys. Res.*, 67: 2777-2779.
- Aubrey, D.G. and Trowbridge, J.H., 1985. Kinematic and dynamic estimates from electromagnetic current meter data. *J. Geophys. Res.*, 90: 9137-9146.
- Basco, D.R., 1982. Surf zone currents — state of knowledge. *Coastal Eng. Res. Cen. Misc. Rep. 82-7 I*, 243 pp.
- Basco, D.R., 1983. Surf zone currents. *Coastal Eng.*, 7: 331-355.
- Bowen, A.J., 1969. Rip currents, 1. Theoretical investigations. *J. Geophys. Res.*, 74: 5467-5478.
- Bowman, D., 1981. Transformational patterns of subaerial micro-tidal beach profiles. *Phys. Geogr.*, 2: 34-46.
- Bowman, D., Arad, D., Rosen, D., Kit, E., Goldbery, R. and Slavicz, A., 1982. Flow characteristics along the rip current system under low energy conditions. *Mar. Geol.* (in prep).
- Clifton, H.E., 1976. Wave formed sedimentary structures, a conceptual model. *Soc. Econ. Paleontol. Mineral., Spec. Publ.*, 24: 126-148.
- Cook, D.O., 1970. The occurrence and geologic work of rip currents off Southern California. *Mar. Geol.*, 9: 173-186.
- Cunningham, P.M., Guza, R.J. and Lowe, R.L., 1979. Dynamic calibration of electromagnetic flow meters. *Inst. Electr. Electron. Eng., Oceans*, 79: 298-301.
- Davidson-Arnott, R.G.D. and Greenwood, B., 1974. Bedforms and structures associated with bar topography in the shallow water environment, Kouchibouguac Bay, New Brunswick, Canada. *J. Sediment. Petrol.*, 44: 698-704.
- Davidson-Arnott, R.G.D. and Greenwood, B., 1976. Facies relationships on a barred coast, Kouchibouguac Bay, New Brunswick, Canada. In: R.A. Davis and R.L. Ethington (Editors), *Beach and Nearshore Sedimentation*. *Soc. Econ. Paleontol. Mineral., Spec. Publ.*, 24: 140-168.
- Dean, R.G., 1973. Heuristic models of sand transport in the surf zone. *Proc. Conf. Engineering Dynamics in the surf zone*, Sydney, N.S.W., 239 pp.
- Draper, L. and Dobson, P.J., 1965. Rip currents on a Cornish beach. *Nature*, 20: 1249.
- Goldsmith, V., Bowman, D. and Kiley, K., 1982. Sequential stage development of crescentic bars: Hahoterim beach, Southeastern Mediterranean. *J. Sediment. Petrol.*, 52: 233-249.
- Greenwood, B. and Davidson-Arnott, R.G.D., 1975. Marine bars and nearshore sedimentary processes, Kouchibouguac Bay, New Brunswick. In: J. Hails and A. Carr (Editors), *Nearshore Sediment Dynamics and Sedimentation*. Wiley Interscience, London, pp.123-150.
- Greenwood, B. and Davidson-Arnott, R.G.D., 1979. Sedimentation and equilibrium in wave formed bars: A review and case study. *Can. J. Earth. Sci.*, 16: 312-332.
- Greenwood, B. and Hale, P.B., 1980. Depth of activity, sediment flux and morphological change in the barred nearshore environment. In: S.B. McCann (Editor), *The Coastline of Canada*. *Geol. Surv. Can.*, 80 (10): 89-109.
- Greenwood, B. and Sherman, D.J., 1984. Wave currents, sediment flux and morphological response in a barred nearshore system. *Mar. Geol.*, 60: 31-61.
- Guza, R.T. and Inman, D.L., 1975. Edge waves and beach cusps. *J. Geophys. Res.*, 80: 2997-3012.
- Guza, R.T. and Thornton, E.B., 1980. Local and shoaled comparisons of sea surface elevations, pressures and velocities. *J. Geophys. Res.*, 85: 1524-1530.
- Hjulstrom, F., 1935. Studies of the morphological activity

- of rivers as illustrated by the river Fyris. *Bull. Geol. Inst. Univ. Uppsala*, 25: 221–527.
- Holman, R.A., 1981. Infragravity energy in the surf zone. *J. Geophys. Res.*, 86: 6442–6450.
- Huntley, D.A. and Bowen, A.J., 1973. Field observations of edge waves. *Nature*, 243: 160–162.
- Huntley, D.A. and Bowen, A.J., 1975. Field observations of edge waves and their effect on beach material. *J. Geol. Soc. London*, 131: 69–81.
- Kit, E., Rosen, D.S., Slavicz, A. and Bowman, D., 1985. Analysis of Current Data. Coastal Mar. Eng. Res. Inst., Technion City, Haifa, P.N.145/85, 684 pp.
- Komar, P.D. and Miller, M.C., 1975. Sediment threshold under oscillatory waves. *Proc. Int. Conf. Coastal Eng.*, 14th, Copenhagen, pp.756–775.
- Leblond, P.H. and Tang, C.L., 1974. On energy coupling between waves and rip currents. *J. Geophys. Res.*, 76: 811–816.
- Lenhart, R.J., 1979. Nearshore marine bedforms, formative processes, distribution and internal structures. Ph.D. thesis, Univ. Cincinnati, Cincinnati, 166 pp.
- McKenzie, P., 1958. Rip current systems. *J. Geol.*, 66: 103–113.
- Noda, E.K., 1974. Wave induced nearshore circulation. *J. Geophys. Res.*, 79: 4097–4106.
- Sasaki, T. and Horikawa, K., 1975. Nearshore current system on a gently sloping bottom. *Coastal Eng. Jpn*, 18: 123–142.
- Shepard, F.P. and Inman, D.L., 1950. Nearshore circulation related to bottom topography and wave refraction. *Eos, Trans. Am. Geophys. Union*, 31: 555–565.
- Shepard, F.P., Emery, K.O. and LaFond, E.C., 1941. Rip currents: A process of geological importance. *J. Geol.*, 49: 337–369.
- Short, A.D., 1979. Wave power and beach stages. A global model. *Proc. Int. Conf. Coastal Eng.*, 16th, Hamburg, pp.1145–1162.
- Short, A.D., 1985. Rip current type, spacing and persistence, Narrabeen beach, Australia. *Mar. Geol.*, 65: 47–71.
- Sonu, C.J., 1972. Field observation of nearshore circulation and meandering currents. *J. Geophys. Res.*, 77: 3232–3247.
- Thornton, E.B., 1979. Energetics of breaking waves within the surf zone. *J. Geophys. Res.*, 84: 4931–4938.
- Vos, R.G., 1976. Observations on the formation and location of transient rip currents. *Sediment. Geol.*, 16: 15–19.
- Wright, L.D., 1982. Field observations of long period surf zone oscillations in relation to contrasting beach morphologies. *Aust. J. Mar. Freshwater Res.*, 33: 181–201.
- Wright, L.D. and Short, A.D., 1983. Morphodynamics of beaches and surf zones in Australia. In: P.D. Komar (Editor), *Handbook of Coastal Processes and Erosion*. CRC Press, Boca-Raton, Fla., pp.35–64.
- Wright, L.D. and Short, A.D., 1984. Morphodynamic variability of surf zones and beaches: A synthesis. *Mar. Geol.*, 56: 93–118.
- Wright, L.D., Chappell, J., Thom, B.G., Bradshaw, M.P. and Cowell, P., 1979a. Morphodynamics of reflective and dissipative beach and inshore systems: Southeastern Australia. *Mar. Geol.*, 32: 105–140.
- Wright, L.D., Thom, B.G. and Chappell, J., 1979b. Morphodynamic variability of high energy beaches. *Proc. Int. Conf. Coastal Eng.*, 16th, Hamburg, pp.1180–1194.
- Wright, L.D., Guza, R.T. and Short, A.D., 1982. Dynamics of a high energy dissipative surf zone. *Mar. Geol.*, 45: 41–62.
- Wright, L.D., Short, A.D. and Green, M.O., 1985. Short-term changes in the morphodynamic states of beaches and surf zones: An empirical predictive Model. *Mar. Geol.*, 62: 339–364.
- Wright, L.D., Nielsen, P., Shi, N.C. and List, J.H., 1986. Morphodynamics of a bar-trough surf zone. *Mar. Geol.*, 70: 251–285.